1 **Epitranscriptomic addition of m^{6}A regulates HIV-1 RNA stability and alternative**

2 **splicing**

3

4 Kevin Tsai[1], Hal P. Bogerd[1], Edward M. Kennedy[1,4], Ann Emery[2], Ronald Swanstrom[2,3]

5 and Bryan R. Cullen[1,*]

6

7 [1] Department of Molecular Genetics and Microbiology, Duke University Medical Center,

8 Durham, NC 27710

9 [2] Lineberger Comprehensive Cancer Center, University of North Carolina at Chapel Hill,

10 Chapel Hill, NC 27599

11 [3] Department of Biochemistry and Biophysics, University of North Carolina at Chapel Hill,

12 Chapel Hill, NC 27599

13 [4] Current address: Oncorus, 50 Hampshire Street, Suite 401, Cambridge, MA 02139

14 [*] Lead Contact

15 Correspondence: bryan.cullen@duke.edu. Tel; 919-684-3369

16

17 Key words: RNA, epitranscriptomic regulation, YTHDF2, YTHDC1, HIV-1, splicing,

18 RNA stability.

19

20 Short Title: Epitranscriptomic regulation of HIV-1 RNA expression

21

22

Abstract

Previous work in several laboratories has demonstrated that the epitranscriptomic addition of m^{6}A to viral transcripts promotes the replication and pathogenicity of a wide range of DNA and RNA viruses, yet the underlying mechanisms responsible for this positive effect have remained unclear. It is known that m^{6}A function is largely mediated by cellular m^{6}A binding proteins or readers, yet how m^{6}A readers regulate viral gene expression in general, and HIV-1 gene expression in particular, has been controversial. Here, we confirm that m^{6}A addition indeed regulates HIV-1 RNA expression and demonstrate that this effect is in large part mediated by the the nuclear m^{6}A reader YTHDC1 and the cytoplasmic m^{6}A reader YTHDF2. Both YTHDC1 and YTHDF2 bind to multiple distinct and overlapping sites on the HIV-1 RNA genome, with YTHDC1 recruitment serving to regulate the alternative splicing of HIV-1 RNAs while YTHDF2 binding correlates with increased HIV-1 transcript stability.

Author Summary

This manuscript reports that the expression of mRNAs encoded by the pathogenic human retrovirus HIV-1 is regulated by the methylation of a small number of specific adenosine residues. These in turn recruit a nuclear RNA binding protein, called YTHDC1, which modulates the alternative splicing of HIV-1 transcripts, as well as a cytoplasmic RNA binding protein, called YTHDF2, which stabilizes viral mRNAs. The regulation of HIV-1 gene expression by adenosine methylation is therefore critical for the effective and ordered expression of HIV-1 mRNAs and could represent a novel target for antiviral development.

2

Introduction

45

46   Eukaryotic mRNAs are subject to a range of covalent modifications at the

47   nucleotide level, collectively referred to as epitranscriptomic modifications. The most

48   common epitranscriptomic modification of mammalian mRNAs is methylation of the N^6

49   position of adenosine, referred to as m^6A, which comprises ~0.4% of all adenosines [1, 2].

50   m^6A residues are deposited on mRNAs by a "writer" complex, minimally consisting of

51   METTL3, METTL14 and WTAP, which adds m^6A to some, but not all, copies of the RNA

52   motif 5'-RRACH-3' (R=G/A, H=A/U/C) [3-6]. Cells also express two demethylases or

53   "erasers", called FTO and ALKBH5, which have been proposed to dynamically regulate

54   m^6A levels [7, 8]. Finally, the phenotypic effects of m^6A on mRNA metabolism are largely

55   conferred by m^6A binding proteins, referred to as m^6A readers, that regulate several steps

56   of RNA metabolism. These include the nuclear m^6A reader YTHDC1, which has been

57   reported to regulate cellular mRNA splicing and nuclear export, and the cytoplasmic m^6A

58   readers YTHDF1, YTHDF2 and YTHDF3, which are thought to regulate the translation

59   and stability of m^6A-containing mRNAs [9-12]. Recent reports suggest that the cytosolic

60   readers YTHDF1, 2 and 3 confer redundant functions, with YTHDF2 the dominant reader

61   due to its higher expression level [13, 14].

62   While m^6A is the most common epitranscriptomic modification on cellular

63   mRNAs, analysis of the genomic RNAs encoded by retroviruses revealed an even higher

64   level of m^6A on these transcripts, with m^6A comprising as much as ~2.4% of the

65   adenosines found on murine leukemia virus (MLV) genomic RNAs [15]. This high

66   prevalence suggests that m^6A might be acting to promote some aspect(s) of the viral

67   replication cycle. Indeed, addition of m^6A has now been shown to boost the replication of

3

68   a diverse range of viruses, including not only MLV but also influenza A virus (IAV), SV40,

69   human metapneumovirus (HMPV), enterovirus 71 and respiratory syncytial virus (RSV)

70   [16]. In the case of IAV, HMPV and RSV, the presence of m6A residues on viral transcripts

71   was also shown to boost pathogenicity *in vivo*. Similarly, for HIV-1, knock down of the

72   m6A writers METTL3 and METTL14 inhibits HIV-1 gene expression and replication while

73   knock down of the m6A erasers FTO or ALKBH5 had the opposite effect [17, 18].

74   However, the mechanism by which this positive effect is achieved has remained

75   controversial. One group [18] reported that a key adenosine residue in the HIV-1 Rev

76   Response Element (RRE) is methylated to m6A and that this m6A residue promotes Rev

77   binding. However, we and others [17, 19-21] have been unable to confirm the presence of

78   any m6A residues on the RRE.

79   Previously, we reported [20] that the cytoplasmic m6A readers YTHDF1, YTHDF3

80   and especially YTHDF2 all promote HIV-1 gene expression and replication yet another

81   group [17, 22] has argued that these same proteins bind to HIV-1 genomic RNAs and are

82   then packaged into virions where they act to inhibit reverse transcription. In contrast, a

83   third group has recently reported that while YTHDF3 is selectively incorporated into HIV-

84   1 virions, it is then inactivated by cleavage by the viral protease. Only when cleavage by

85   the HIV-1 protease was inhibited was YTHDF3 found to exert an inhibitory effect [23].

86   Here, we have sought to more fully define how m6A residues interact with cellular readers

87   to positively affect HIV-1 mRNA function and report that m6A promotes HIV-1 gene

88   expression by at least two distinct mechanisms. On the one hand, m6A assures the optimal

89   alternative splicing of HIV-1 transcripts by recruiting the nuclear m6A reader YTHDC1.

4

90   On the other hand, m^{6}A also enhances the stability of viral mRNAs by recruiting the

91   cytoplasmic m^{6}A reader YTHDF2.

92

93   **Results**

94   *Removal of m^{6}A residues reduces the level of HIV-1 RNA expression*

95   Previously, it has been demonstrated that knock down of the m^{6}A writers METTL3

96   and METTL14 using RNA interference (RNAi) inhibits HIV-1 Gag expression while

97   knock down of the m^{6}A erasers ALKBH5 or FTO increases HIV-1 Gag expression [17,

98   18], yet the molecular basis for this positive effect of the m^{6}A modification has remained

99   unclear. As an alternative approach, we overexpressed the m^{6}A eraser ALKBH5, which

100   has been previously demonstrated to globally reduce m^{6}A levels on RNA [7, 24]. A

101   lentiviral ALKBH5 expression vector was used to transduce the CD4$^+$ T cell line CEM and

102   three single cell clones were isolated, each expressing an ~3-fold higher level of ALKBH5

103   than the parental cells (Figs. 1A and 1B). To confirm m^{6}A depletion on mRNAs expressed

104   in these ALKBH5 over-expressing cells (+ALKBH5), we quantified the m^{6}A content of

105   purified poly(A)$^+$ RNA extracted from HIV-1 infected parental or +ALKBH5 CEM cells

106   at 3 days post-infection (dpi) using an m^{6}A ELISA assay. Isolation of poly(A)$^+$ RNA by

107   oligo-dT purification successfully removed >90% of rRNA (Fig. S1) and we observed that

108   poly(A)+ RNA isolated from the +ALKBH5 CEM cells contained ~50% less m^{6}A than

109   WT CEM cells (Fig. 1C).

110   We next infected WT and +ALKBH5 CEM cells with HIV-1 and then limited this

111   infection to a single cycle by addition of the reverse transcriptase (RT) inhibitor nevarapine

112   at 16 hours post-infection (hpi), followed by harvest at 48 hpi for analysis of viral gene

113 expression. In all three +ALKBH5 clones, reduced m^{6}A addition resulted in not only a

114 ~60% drop in viral Gag protein expression (Figs. 1A and D) but also a similar ~60% drop

115 in the level of both unsliced and spliced HIV-1 transcripts (Fig. 1E). These data indicate

116 that m^{6}A addition to HIV-1 mRNAs results in enhancement of HIV-1 gene expression at

117 the RNA level.

118

119 *YTHDF2 binding stabilizes HIV-1 mRNAs*

120 As noted above, while we have previously reported that the cytoplasmic m^{6}A

121 readers YTHDF1, YTHDF2 and YTHDF3 increase HIV-1 gene expression and replication,

122 others have argued that they exert an inhibitory effect [17, 20]. As it has recently been

123 reported that all three YTHDF proteins function by similar mechasnisms [13], and because

124 YTHDF2 is the most highly expressed variant in T cells [20], we focused on this cellular

125 protein. We first sought to confirm that YTHDF2 can indeed enhance viral replication by

126 transfecting 293T cells with a plasmid expressing the HIV-1 receptor CD4, along with

127 either an empty plasmid (Ctrl) or a plasmid expressing YTHDF2 (+DF2), and confirmed

128 that this results in YTHDF2 overexpression (Fig. 2A). Control and YTHDF2

129 overexpressing cells were then infected with a fully replication competent HIV-1 variant

130 expressing nano luciferase (NLuc) in place of Nef. At 24 hpi we observed a significant, ~3

131 fold increase in total viral RNA expression in the +DF2 cells when compared to Ctrl cells

132 (Fig. 2B). Analysis of virally-encoded NLuc expression at 24 and 48 hpi revealed an ~4

133 fold higher level of NLuc expression at 24 hpi and demonstrated that this indicator virus

134 was, as expected, able to effectively spread through the CD4+ 293T cell culture while

135 maintaining the higher level of NLuc expression seen at 24 hpi.

6

136   As noted above, one group has reported that all three cytoplasmic YTHDF readers

137   are incorporated into HIV-1 virions, where they act to inhibit reverse transcription, while

138   a second group has reported that virion packaging is specific for YTHDF3, which is then

139   degraded by the viral protease [17, 22, 23]. To determine whether the YTHDF proteins are

140   indeed incorporated into HIV-1 virions, we co-transfected 293T cells with a molecular

141   clone of HIV-1 along with vectors expressing either FLAG-tagged forms of the m^6A

142   readers YTHDF1, 2 or 3 or expressing FLAG-tagged African green monkey APOBEC3G

143   (agmA3G), which is known to be packaged into virions [25-27]. While all three YTHDF

144   proteins, along with agmA3G, were detected at comparable levels in virus-producing cells

145   (Fig. 2D, upper panel), only agmA3G was detected in highly purified virion particles

146   isolated from the supernatant media by centrifugation through a sucrose cushion followed

147   by banding on an iodixanol gradient (Fig. 2D, center panel). The failure to detect virion-

148   packaged m^6A readers could not be explained by their HIV-1 protease-mediated

149   degradation, as the virions were prepared in the presence of the viral protease inhibitor

150   indinavir, as confirmed by the fact that only full length, p55 Gag was detected in these

151   virions (Fig. 2D, lower panel)

152   We next sought to more precisely define the mechanism by which YTHDF2

153   enhances HIV-1 gene expression using a more biologically relevant system, ie. single cycle

154   infection by HIV-1 of the CD4$^+$ T cell line CEM-SS. YTHDF2 knockout (ΔDF2) or

155   wildtype (WT) CEM-SS cells, and YTHDF2-overexpressing (+DF2) or GFP-expressing

156   (+GFP) CEM-SS cells, have been previously described [20]. WT/ΔDF2 and +GFP/+DF2

157   CEM-SS cells were infected with HIV-1, RT blocked at 16 hpi using nevarapine to ensure

158   a single cycle infection, and then harvested at 48 hpi. We observed both reduced Gag

159   protein expression in the ΔDF2 cells as well as increased Gag expression in the +DF2 cells,

160   confirming that YTHDF2 indeed enhances viral gene expression in a single-cycle non-

161   spreading infection of T cells (Fig. 3A and 3B). We also observed an ~80% drop in viral

162   RNA levels in the ΔDF2 cells and an ~80% increase in viral RNA in the infected +DF2

163   CEM-SS cells, respectively, when compared to control cells (Fig. 3C), again suggesting

164   that YTHDF2 upregulates viral gene expression at the RNA level. YTHDF2 has been

165   reported to be cytosolic [9] , which we confirmed in the CEM-SS T cell line (Fig. S3A)

166   and we therefore hypothesized that YTHDF2 was likely regulating HIV-1 RNA stability

167   rather than synthesis. To test this, we again performed a single cycle infection of the WT

168   and ΔDF2 CEM-SS cells but added the transcription inhibitor Actinomycin D (ActD) at

169   48 hpi. HIV-1 RNA levels were then quantified by qRT-PCR at multiple time points to

170   monitor the rate of RNA decay. We indeed observed a significantly faster decay of HIV-1

171   transcripts in the ΔDF2 cells, when compared to WT CEM-SS cells (Fig. 3D), while no

172   difference was observed for a previously reported m^6A-free host transcript called NONO

173   (Fig. 3E) [1]. These data indicate that YTHDF2 boosts HIV-1 gene expression by

174   enhancing the stability of m^6A^+ viral RNA.

175

176   *Both YTHDC1 and YTHDF2 bind to m^6A sites on HIV-1 transcripts.*

177   HIV-1 replication is tightly regulated by a remarkably complex pattern of

178   alternative splicing that results in the ordered expression of up to 30 unspliced, partially

179   spliced and fully spliced viral mRNAs [28, 29]. Both m^6A and the nuclear m^6A reader

180   YTHDC1 have been reported to affect cellular mRNA splicing [1, 10] and we therefore

181   sought to determine if HIV-1 RNA splicing is also epitranscriptomically regulated by

8

182 YTHDC1 binding to viral m6A residues. Initially, we used the photo-assisted cross linking

183 and immunoprecipitation (PAR-CLIP) technique [30] to map YTHDC1 binding sites on

184 HIV-1 transcripts in infected cells and compared these to the previously mapped binding

185 sites for YTHDF1 and YTHDF2 as well as sites of m6A addition mapped by antibody

186 binding (PA-m6A–seq, Fig. 4) [19, 20]. We identified at least 7 reproducible YTHDC1

187 binding sites across two independent PAR-CLIP experiments, and found that these largely

188 coincided with previously mapped sites of m6A addition [19] as well as with known

189 YTHDF1 and YTHDF2 binding sites [20]. Moreover, these sites all contained the m6A

190 addition motif 5'-RRACH-3' [1, 2]. Due to splicing, the read depth in the first ~7500nt of

191 the viral genome is markedly lower than in the 3' untranslated region of viral mRNAs in

192 infected cells. Nevertheless, we were able to map a YTHDC1 binding site adjacent to HIV-

193 1 splice acceptor A3 (Fig. 4A), as well as a binding site overlapping splice acceptor A7

194 (Fig. 4B), in addition to YTHDC1 binding sites coincident with the previously reported

195 m6A sites in the *env/rev* overlap, the *nef* gene and in the TAR hairpin [20]. Conversely, the

196 m6A sites at ~8,900 nt located in the NF-kB sites in the viral LTR U3 region are at best

197 weakly bound by YTHDC1 (Fig. 4B). Of note, we observed no binding of YTHDC1,

198 YTHDF1, YTHDF2 or the m6A-specific antibody to the reported m6A addition site in the

199 RRE [18], which agrees with m6A mapping data on HIV-1 RNAs reported by others [17].

200

201 *YTHDC1 regulates the expression of HIV-1 transcripts*

202   Having confirmed that YTHDC1 indeed binds m6A residues on HIV-1 transcripts

203 in infected cells, we next asked whether YTHDC1 can regulate HIV-1 RNA expression.

204 Because we were unable to obtain YTHDC1 knockout cells, implying that YTHDC1 may

9

205 be an essential gene, we instead used RNAi to knockdown YTHDC1 expression. We

206 transfected 293T cells with a plasmid encoding the HIV-1 receptor CD4 and also

207 transfected the cells on two successive days with siRNAs targeting YTHDC1 mRNA

208 (siDC1) or with control siRNAs (siCtrl). As expected, we observed a decrease in YTHDC1

209 protein expression only in the siDC1 transfected cells and this correlated with a surprising

210 increase in HIV-1 Gag protein expression (Fig. 5A, lanes 1-3). If the increase in viral Gag

211 expression is indeed a direct consequence of reduced YTHDC1 expression, then one might

212 predict a decrease in viral Gag expression upon overexpression of YTHDC1 (+DC1), and

213 this was indeed observed (Fig. 5A, compare lanes 4 and 5). A similar effect was seen at the

214 RNA level, with quantification of total, unspliced and spliced viral RNA (specifically viral

215 RNAs spliced from D1 to A1) using qRT-PCR revealing that knock down of YTHDC1

216 using RNAi resulted in a significantly higher level of viral RNA expression, whereas

217 YTHDC1 overexpression resulted in reduced viral RNA expression (Fig. 5B). This effect

218 was not observed for the NONO transcript lacking m^6A sites and was more prominent for

219 the spliced viral RNA bearing the D1/A1 splice junction than for the unspliced viral RNA,

220 thus suggesting that the nuclear YTHDC1 protein (Fig. S2B) might regulate HIV-1 RNA

221 expression post-transcriptionally.

222

223 *YTHDC1 does not regulate the nuclear export of HIV-1 transcripts*

224   YTHDC1 has been proposed to regulate both the alternative splicing and nuclear

225 export of cellular m^6A methylated mRNAs [10, 12] and we first asked whether YTHDC1

226 might regulate the nuclear export of HIV-1 transcripts. To determine whether knock down

227 of YTHDC1 expression had any effect on the nucleocytoplasmic localization of either fully

10

228   spliced or incompletely spliced HIV-1 RNAs, we isolated nuclear or cytoplasmic fractions

229   from WT or YTHDC1 knock down 293T cells. Analysis of these fractions by Western

230   analysis for the nuclear protein Lamin or the cytoplasmic protein GAPDH confirmed the

231   integrity of the fractionation process and further confirmed not only the nuclear localization

232   of YTHDC1 but also the effective knock down of YTHDC1 protein expression by RNAi

233   (Fig. 5C). Analysis of viral RNA expression in the isolated nuclear and cytoplasmic

234   fractions confirmed that knock down of YTHDC1 expression substantially enhanced the

235   expression of HIV-1 transcripts bearing the D1/A1 splice junction (Figs. 5D and E), as

236   previously noted in total cellular RNA (Fig. 5B). However, this analysis did not reveal any

237   changes in the subcellular localization of either unspliced viral RNA, or fully spliced viral

238   RNAs bearing the D4/A7 splice junction, when YTHDC1 expression was inhibited (Fig.

239   5D-F).

240

241   *YTHDC1 regulates the alternative splicing of HIV-1 transcripts*

242   The observation that knock down of YTHDC1 expression using RNAi strongly

243   enhanced the expression of HIV-1 transcripts bearing the D1/A1 splice junction, while only

244   modestly affecting both unspliced and total viral RNA expression (Fig. 5) suggested that

245   YTHDC1 might regulate the alternative splicing of HIV-1 transcripts, as has indeed been

246   previously proposed for cellular RNAs [10]. To determine whether this is the case, we used

247   Primer-ID-based deep sequencing of splice forms [31] to quantitatively measure the effect

248   of YTHDC1 on HIV-1 alternative splicing. In this assay, a common forward primer that

249   anneals 5' to the *gag* gene can be paired with either random reverse primers, or splice form-

250   specific 4kb or 1.8kb reverse primers, to selectively amplify viral transcripts (Fig. 6A).

251   HIV-1 transcripts are divided by size into the ~9kb unspliced transcript, ~4kb incompletely

252   spliced transcripts (which retain the D4/A7 *env* intron), and ~1.8kb fully spliced transcripts,

253   (lacking the D4/A7 intron). While the random reverse primer amplifies all viral transcripts,

254   the 4kb reverse primer, located within the D4/A7 intron, only amplifies incompletely

255   spliced transcripts. The 1.8kb reverse primer spans the D4/A7 splice junction and thus only

256   amplifies fully spliced transcripts. Using the random reverse primer, we first noted that

257   ~33% of viral transcripts are spliced in the siCtrl cells, while this increased to ~42% in the

258   siDC1 cells but decreased to ~25% in the +DC1 cells (Fig. 6B). Yet, among spliced

259   transcripts, a constant ~85% of all spliced transcripts were fully spliced, that is lacking the

260   D4/A7 intron, regardless of YTHDC1 expression level (Fig. 6C). Thus, YTHDC1 has a

261   stronger inhibitory effect on utilization of splice donor D1 than D4. Quantification of the

262   level of splicing between donor D1 and the central splice acceptors A1-A5 (Fig. 6D), using

263   the random reverse primer, revealed that YTHDC1 overexpression led to a significant bias

264   towards utilization of the more 3' acceptors A3, A4 and A5, at the expense of the more 5'

265   acceptors A1 and A2 (Fig. 6D) and, as expected, the opposite result was observed in cells

266   in which YTHDC1 expression was knocked down, ie. increased utilization of A1 and A2

267   and a concomitant reduction in the utilization of A3, A4 and A5. The class-specific 1.8 and

268   4kb reverse primers confirmed this bias (Figs. 6E and F). YTHDC1 over-expression also

269   led to a significant, ~2.5x increase in the detection of the normally very rare D1 to A7

270   splice (Fig. 6G), consistent with the observed bias towards splicing D1 to more 3' splice

271   acceptors in YTHDC1 overexpressing cells. Finally, we noted that among the transcripts

272   that used splice acceptor A2, YTHDC1 significantly decreased the proportion of viral

12

273   RNAs that were additionally spliced using splice donor D3 (Fig. 6H), thus incorporating

274   the small non-coding exon located between A2 and D3 (Fig. 6A).

275

Discussion

277   Previously, knock down of the m^{6}A writers METTL3 and METTL14 using RNAi

278   was reported to inhibit HIV-1 gene expression, while knock down of the m^{6}A erasers FTO

279   and ALKBH5 enhanced HIV-1 gene expression [17, 18]. The resultant conclusion that

280   m^{6}A must facilitate one or more aspects of the HIV-1 replication cycle is consistent with

281   the finding that HIV-1 genomic RNAs contain higher levels of m^{6}A than the average

282   cellular mRNA [19]. More recently, m^{6}A was shown to enhance the replication and

283   pathogenicity of a wide range of DNA and RNA viruses [16], thus implying that the

284   underlying mechanism of action of m^{6}A, though still unclear, positively affects the

285   expression and/or function of a range of viral RNA transcripts.

286   In one early study looking at how m^{6}A promotes HIV-1 gene expression, a key

287   adenosine residue on the RRE was proposed to be methylated to m^{6}A and then promote

288   Rev binding and HIV-1 RNA nuclear export [18]. However, several later studies failed to

289   detect any m^{6}A residues on the RRE [17, 19, 20] and the presence or absence of m^{6}A at

290   this RRE residue was found to not, in fact, affect Rev binding [21]. Moreover, as the

291   expression of mRNAs encoded by several cytoplasmic RNA viruses is also boosted by

292   m^{6}A addition [16], nuclear RNA export cannot be the primary mechanism of action of

293   m^{6}A.

294   While m^{6}A has the potential to affect RNA secondary structure, it is nevertheless

295   clear that the phenotypic consequences of m^{6}A addition are largely mediated by m^{6}A

13

296   readers, which include the nuclear m^6A reader YTHDC1 and the cytoplasmic m^6A readers

297   YTHDF1, YTHDF2 and YTHDF3. While we have previously reported that all of the

298   cytoplasmic readers, including especially YTHDF2, significantly boost HIV-1 RNA

299   expression in infected cells [20], others have proposed that the YTHDF proteins are bound

300   to m^6A residues on the HIV-1 genomic RNA and then packaged into HIV-1 virions where

301   they act to inhibit reverse transcription [17]. This latter result is clearly inconsistent with

302   the finding, by this group and others [17, 18, 20], that m^6A strongly promotes HIV-1

303   replication. Moreover, as m^6A is added to RNAs at the consensus sequence 5'-RRACH-

304   3', mutants lacking this motif should be rapidly selected during passage of a rapidly

305   replicating, error prone RNA virus such as HIV-1 if m^6A indeed exerted an inhibitory effect

306   in *cis*. Recently it was been reported that, if YTHDF proteins are indeed packaged into

307   HIV-1 virions, then they are effectively inactivated due to degradation by the viral protease

308   [23]. However, we were unable to detect the virion packaging of any YTHDF reader

309   protein even when viral protease activity was inhibited (Fig. 2D).

310   In this report, we have sought to define the precise step(s) in the HIV-1 replication

311   cycle that is regulated by m^6A-bound reader proteins. In the case of YTHDF2, we show

312   that this reader primarily acts to increase HIV-1 RNA expression, and not translation, and

313   demonstrate that this effect is mediated by enhanced viral RNA stability (Fig. 2 and 3) This

314   is a surprising result given that most previous studies looking at YTHDF2 function have

315   reported that YTHDF2 binding to cellular mRNAs actually destabilizes the RNA [9, 32],

316   although several reports have suggested that m^6A can stabilize cellular transcripts in some

317   cases [33] with one report demonstrating that m^6A addition stabilizes specific cellular

318   mRNAs during hypoxia [34]. We also note that m^6A is known to promote the expression

14

319 of mRNAs encoded by a wide range of viruses [16], which is clearly inconsistent with the

320 idea that the recruitment of cytoplasmic readers inhibits mRNA expression. Why

321 YTHDF2, and potentially the other cytoplasmic m^6A readers, stabilize m^6A-containing

322 viral RNAs yet destabilize most m^6A-containing cellular RNAs is currently unknown,

323 though it appears possible that this is dependent on the simultaneous recruitment of other

324 RNA binding proteins that remain to be identified, perhaps to adjacent sites on the viral

325 RNA. We note that the inhibitory effect on HIV-1 gene expression in infected T cells seen

326 when expression of the YTHDF2 reader is blocked (Fig. 3) is indistinguishable from the

327 inhibitory effect seen when removal of m^6A residues from viral transcripts is enhanced by

328 overexpression of the m^6A eraser ALKBH5 (Fig. 1), thus arguing that the boost in total

329 viral RNA expression that results from the addition of m^6A residues is largely mediated by

330 cytoplasmic RNA readers.

331 While there has been little previous work looking at the effect of m^6A on viral RNA

332 splicing, with the exception of a recent paper showing that depletion of the m^6A writer

333 METTL3 reduces the efficiency of splicing of adenoviral late mRNAs [35], it is known

334 that m^6A addition can regulate cellular mRNA splicing, acting predominantly via the

335 nuclear m^6A reader YTHDC1 [1, 10, 36, 37]. As HIV-1 transcripts are among the most

336 extensively alternatively spliced RNAs ever identified [29, 38], we were interested in

337 whether YTHDC1 regulated this process in infected cells. Using the PAR-CLIP technique,

338 we were indeed able to map at least 7 distinct YTHDC1 binding sites on HIV-1 transcripts

339 that largely, but not entirely, coincided with previously mapped YTHDF1 and YTHDF2

340 binding sites as well as sites of m^6A addition previously mapped using the antibody-

341 dependent technique PA-m^6A-seq [19, 20] (Fig. 4). As we were unable to knock out

15

342   YTHDC1 using CRISPR/Cas, we decided to knock down YTHDC1 expression using

343   RNAi, and also overexpress YTHDC1 by transfection, to determine whether changing the

344   level of YTHDC1 expression affected HIV-1 RNA expression and/or alternative splicing.

345   As shown in Figs. 5A and B, we unexpectedly observed that knock down of YTHDC1

346   actually increased HIV-1 Gag protein and RNA expression while overexpression of

347   YTHDC1 inhibited HIV-1 gene expression. This effect, which is the exact opposite of what

348   we saw when YTHDF2 was knocked out or overexpressed (Figs 2 and 3), was particularly

349   significant for viral RNAs spliced from donor D1 to acceptor A1 (Fig. 5B), thus suggesting

350   that YTHDC1 indeed regulated some aspect(s) of HIV-1 RNA metabolism. Despite

351   previous reports indicating that YTHDC1 can regulate the nuclear export of cellular

352   mRNAs [12], and our report that m^6A regulates the nuclear export of SV40 transcripts [39],

353   we did not detect any effect of YTHDC1 knock down on the nuclear export of either

354   unspliced HIV-1 transcripts, which is dependent on the viral Rev protein and its cellular

355   cofactor CRM1, or on the subcellular localization of fully spliced viral transcripts bearing

356   the D4/A7 splice junction, which is mediated by the canonical cellular nuclear mRNA

357   export factor NXF1 (Fig. 5) [40]. However, using the previously described "Primer-ID-

358   based deep sequencing of splice forms" technique [31], we were able to document clear

359   and opposite effects of YTHDC1 knock down or overexpression on the relative utilization

360   of specific HIV-1 splice acceptors. Specifically, knock down of YTHDC1 modestly

361   increased viral RNA splicing (Fig. 6B) by increasing the utilization of splice acceptors A2

362   and particularly A1, while simultaneously reducing the utilization of splice acceptors A3,

363   A4 and A5 (Figs. 6D-F), thus explaining the increased level of D1 to A1 spliced RNA

364   detected by qRT-PCR in Fig. 5. Overexpression of YTHDC1, in contrast, reduced

16

365   utilization of A1 and A2 while simultaneously increasing the utilization of acceptors A3,

366   A4 and A5, an effect that was most clearly seen when the random reverse primer splicing

367   assay was used (Fig. 6D).

368   Previous work looking at the effect of YTHDC1 on splicing of cellular mRNAs

369   largely looked at the effect of YTHDC1 on the inclusion or skipping of cassette exons and

370   concluded that YTHDC1 promoted exon inclusion by recruiting the pre-mRNA splicing

371   factor SRSF3 [10]. However, this report did not address whether the location of m^{6}A

372   addition sites relative to splice sites was important. As alternative splicing of HIV-1 RNAs

373   is a much more complex process than simple exon inclusion or exclusion, it is hard to

374   address whether our data are consistent with this earlier report. However, we note that none

375   of the mapped YTHDC1 binding sites on the HIV-1 genome colocalize with either known

376   viral splicing enhancer/repressor elements or with any intronic branch points (consensus

377   motif 5'-YNYURAY-3') [41]. A minor peak of YTHDC1 binding does precisely overlap

378   with splice acceptor A7, with the only m^{6}A motif present in this peak (5'-RRm^{6}ACH-3')

379   positioning the splice junction exactly 5' to the m^{6}A (Fig. 4B). YTHDC1 overexpression

380   also biases D1-originating splices away from acceptors A1 and A2, and towards A3, A4,

381   A5 and A7 (Fig. 6) and we mapped a YTHDC1 binding site between A2 and A3 (Fig. 4A),

382   which demarcates the border of this effect. However, determining whether the precise

383   location of the YTHDC1 binding sites mapped on the HIV-1 genome, relative to splice

384   sites, is indeed important may be challenging, given the difficulty of generating silent

385   mutations at many of these sites.

386

17

Materials and methods

Cell lines and virus clones

HEK293T cells (referred to as 293T), a human kidney epithelial cell line of female origin, was purchased from the American Type Culture Collection. CEM and CEM-SS cells are human CD4+ T cell lines of female origin, with CEM-SS a subclone of CEM. Both were obtained from the NIH AIDS reagent program. 293T cells were cultured in Dulbecco's Modified Eagle's Medium (DMEM) with 6% fetal bovine serum (FBS) and 1% Antibiotic-Antimycotic (Gibco, 15240062). T cell lines were cultured in Roswell Park Memorial Institute (RPMI) 1640 medium supplemented with 10% FBS and 1% Antibiotic-Antimycotic.

The +ALKBH5 cells were produced by transducing CEM cells with a lentiviral vector expressing FLAG-ALKBH5 followed by puromycin selection and single cell cloning. YTHDF2 knock out and overexpressing CEM-SS cells were previously described [20]. YTHDC1 mRNA knockdown in 293T cells was performed using siRNAs (Origene # SR314128) transfected using Lipofectamine RNAiMax (Invitrogen).

Recombinant virus clones used include the laboratory strain NL4-3, obtained from the NIH AIDS Reagent [42], and the nano-luciferase reporter virus NL4-3-NLuc, in which the viral *nef* gene has been substituted with the NLuc indicator gene [43].

Antibodies

Anti-FLAG (M2), Sigma F1804. Anti-HIV-1 p24 gag #24-3, ARP-6458. Anti-GAPDH, Proteintech 60004-1-Ig. Anti-ALKBH5, Proteintech 16837-1-AP. Anti-

409   YTHDF2, Proteintech 24744-1-AP. Anti-YTHDC1, Abcam ab122340. Anti-mouse IgG,

410   Sigma A9044. Anti-rabbit IgG, Sigma A6154.

411

Cloning of protein expression plasmids

413   ALKBH5 was cloned out of cDNA produced from CEM cells, by PCR with Q5

414   High-Fidelity DNA Polymerase (NEB M0491) and the following primers: 5'-

415   atgGCGGCCGCcagcgg-3' and 5'- aaaCTCGAGtcagtgccgccgcatcttcacc-3' (enzyme

416   digestion sites in capital letters). The 5'end of the ALKBH5 coding regions naturally

417   contains a Not I digestion site while the reverse primer introduces a Xho I site right after

418   the stop codon. This PCR product was subsequently digested with Not I and Xho I, and

419   ligated into the matching digestion sites of the lentiviral vector pLEX-FLAG, which

420   encodes double FLAG tags 5' of the Not I site [20].

421   Similarly, YTHDC1 was cloned out of cDNA by PCR using the primers: 5'-

422   aaaGCGGCCGCtgcggctgacagtcggg-3' and 5'-aaaCTCGAGttatcttctatatcgacctctctcccctc-

423   3' (enzyme digestion sites in capital letters), digested and ligated into the Not I and Xho I

424   sites of pLEX-FLAG, producing pLEX-FLAG-YTHDC1 which encodes an N'-2xFLAG-

425   tagged YTHDC1. This FLAG-YTHDC1 was subsequently PCR clones with primers 5'-

426   aaaAAGCTTatggattataaggatgatgatgataaagg-3'   and   5'-

427   aaaGAATTCttatcttctatatcgacctctctccc-3', then digested with Hind III and Eco RI and

428   ligated into pK-Myc to build the CMV promoter driven expression vector pK-FLAG-

429   YTHDC1.

430

Generation of ALKBH5 overexpression CEM cells

19

432 The lentiviral pLEX-FLAG-ALKBH5 vector was packaged in 293T cells and used

433 to transduce CEM cells. At 3 days post transduction, cells were subject to selection with 2

434 µg/mL puromycin for a week until an accompanying untransduced well of cells was

435 completely dead, then the transduced cells were single cell cloned by limiting dilution.

436 Three clones that strongly expressed a FLAG-ALKBH5 protein band slightly larger then

437 endogenous ALKBH5 were used for downstream assays.

438

439 **YTHDF2 knockout and over-expression cells**

440 CEM-SS cells with YTHDF2 knocked out by CRISPR/Cas9, overexpressing cells

441 from transduction with pLEX-FLAG-YTHDF2, and the corresponding pLEX-FLAG-GFP

442 transduced control cells, were previously characterized [20].

443

444 **Validation of m^{6}A depletion in ALKBH5 over-expression cells**

445 4 million each of WT and +ALKBH5 CEM cells were infected with NL4-3 virus,

446 harvested 3 days post infection (dpi), and total RNA extracted with 1ml of Trizol. 150µg

447 of total RNA from each sample were poly(A) purified twice using the Poly(A)Purist MAG

448 Kit (Invitrogen #AM1922). After the first poly(A) purification, the used oligo-dT beads

449 were kept in PBS in tubes marked with the samples they were used on, and subsequently

450 used for the 2nd round of poly(A) purification of the same samples with 30% fresh beads

451 added. All double poly(A) purified RNAs were normalized to a concentration of 75ng/µl,

452 and 200ng of each sample analyzed for m^{6}A content using the EpiQuik m6A RNA

453 Methylation Quantification ELISA Kit (EpiGentek # P-9005-48). The results were read

454 using a BMG Clariostar plate reader at the Duke Functional Genomics core facility to read

20

455 the absorbance at 450nm. To validate the purity of double poly(A) purified RNA, 75ng

456 each of pre- and post- purification RNA were analyzed on a Agilent Bioanalyzer using the

457 RNA 6000 Nano assay, the default analysis software autodetects and quantifies the bands

458 corresponding to the 18S and 28S rRNA.

459

460 **HIV-1 replication assays in YTHDF2 overexpressing 293T cells**

461 NLuc virus was packaged in 293T cells in 10 cm plates by transfection of 10μg of

462 pNL4-3-NLuc with PEI (polyethylenimine). For infection of target cells, 293T cells in 6

463 well plates were co-transfected with 1μg empty vector or pEFtak-FLAG-YTHDF2 [20]

464 and 0.5μg pCMV-CD4 using PEI, media changed 24hrs post, cells passaged 48hrs post,

465 and infected with NL4-3-NLuc 72hrs post transfection, and harvested 24 or 48hrs post

466 infection. Luciferase assays require washing the harvested cells 3 times in PBS prior to

467 lysis in passive lysis buffer (Promega, E1941). NLuc activity was assayed using the Nano

468 Luciferase Assay Kit (Promega, N1120).

469

470 **YTHDF reader protein virion packaging assay**

471 5μg pNL4-3-NLuc was co-transfected with 5μg of pEFtak-FLAG-YTHDF1,

472 pEFtak-FLAG-YTHDF2, pEFtak-FLAG-YTHDF3, [20] or pCDNA3-FLAG-agmA3G

473 [25] into 293T cells using PEI, and the cells immediatly treated with 5μM of Indinavir. 3

474 days post-transfection, producer cells and supernatant media were collected. The

475 supernatant media wwas passed through a 0.45μm pore size filter, and virions purified by

476 centrifugation through a 20% sucrose cushion, followed by banding on a 6-18% Iodixanol

477 gradient (Sigma D1556) each by 90 mins of ultracentrifugation at 38,000 rpm [19].

21

478   Producer cell pellets and purified virion pellets were then lysed and analyzed by Western

479   blot.

480

Immunofluorscence microscopy

482   0.1 million CEM-SS cells were suspended in 300µl PBS and spun onto glass slides

483   using a Thermo Scientific Shandon Cytospin 4 at 1000rpm 3mins. Slides were then

484   immediately fixed in 2% paraformaldehyde in PBS for 10mins, followed by 2 PBS washes.

485   Cells were then permeabilized in 0.3% Triton-X 100 in PBS for 20mins, and washed twice

486   with PBS, and blocked with 1% BSA in PBS for 45mins. Cells were stained with 1/1000

487   or 1/3000 diluted antibodies targeting YTHDF2 or YTHDC1 (in 1% BSA PBS), over night

488   at 4°C, followed by 3 washes. Cells were then counter stained with 1/1000 diluted

489   Alexafluor 488 (Invitrogen A11034) anti-rabbit, and washed twice with PBS, once each

490   with 70% and 100% EtOH, and air dried briefly. Each cytospin dot was mounted with

491   Vectashield (H1200), pre-mixed with DAPI, and left at -20°C for a few days. Slides were

492   visualized with an EVOS M5000 microscope at 40x magnification.

493

YTHDC1 knockdown and overexpression assays

495   On day 0, 293T cells were seeded at 2 million cells in 8ml DMEM per 10cm plate

496   and 0.4 million cells in 2ml DMEM per 6 well plate well. The next day (day 1), the 10cm

497   plate was transfected with 10µg of pNL4-3 plasmid using PEI. The 6 well plates were used

498   as target cells, with each well transfected with non-targeting (siCtrl) or YTHDC1-targeted

499   siRNAs (siDC1, Origene # SR314128, three YTHDC1 siRNAs premixed at a 1:1:1 ratio):

500   2.5µl of a 2nmol stock siRNA was diluted in 122.5µl of OPTI-MEM (Gibco), and 7.5µl of

22

501   Lipofectamine RNAiMax (Invitrogen) was separately diluted in 117.5µl of OPTI-MEM.

502   The pre-diluted siRNA and Lipofectamine solutions were combined and, 5mins later,

503   added drop-wise to the cells in 6 well plates. 6-8hrs post siRNA transfection, the

504   transfection media was removed from 6 well plates, and the cells overlaid with fresh

505   DMEM. The cells in 6 well plates were subsequently co-transfected with 0.5µg pCMV-

506   CD4, 1.5µg pBC-CXCR4, and 1µg of either empty pK vector or pK-FLAG-YTHDC1,

507   using PEI. On day 2, the media of 10cm and 6 well plates were exchanged for fresh DMEM,

508   and the 6 well plates were subject to a second round of siRNA transfection. The

509   transfections were coordinated for a control well transfected with pK vector + siCtrl, a

510   knockdown well of pK vector + siDC1 and an overexpression well of pK-FLAG-YTHDC1

511   + siCtrl. On day 3, the media was changed again on the 6 well plates to remove the

512   transfection mix. Day 4, the cells in the 6 well plates were trypsinized, counted and seeded

513   either 0.5 million in 0.5ml DMEM per well in 12 well plates or 1 million in 1ml DMEM

514   per well in 6 well plates. The NL4-3 virus-containing supernatant media from the 10cm

515   plates was filtered through a 0.45µm pore size filter to remove any contaminating cells,

516   brought up to 12mls with DMEM, and added to the just seeded infection target cells:

517   2ml/well of virus for infections in 6 well plates, 1ml/well for 12 well plates. To limit to a

518   single cycle infection, infected cells were treated with 133µM of the reverse transcriptase

519   inhibitor Nevirapine (Sigma SML0097) at 16 hpi, then harvested at 48 hpi for protein or

520   RNA analysis. For each experiment, an aliquot of each siRNA/CD4-transfected infection

521   target cells were seeded in a 12 well plate the day of infection for Western blot validation

522   of YTHDC1 knockdown the next day.

523

Subcellular fractionation assays

HIV-1 infected 293T cells, expressing wild type or knocked down levels of YTHDC1, were lysed and divided into nuclear and cytoplasmic fractions as previously described [39].

Single cycle replication assays in T cell lines

These were performed as previously described [44]. Briefly, NL4-3 virus was packaged in 10cm plates of 293T cells, and the culture media exchanged with fresh RPMI media the day after transfection. 3 days post transfection, the virus-containing supernatant media were harvested and filtered through a 0.45μm pore size filter, and the virus-containing filtrate brought up to a total volume of 12 ml with RPMI. The day before infection, infection target cells of interest were passaged to ensure cells were growing healthily. Infection target cells were counted and seeded at 1 million cells per 12 well plate in 0.5ml fresh RPMI, and subsequently overlayed with 1ml of the virus-containing filtrate. To limit to a single cycle infection, infected cells were treated with 133μM of the reverse transcriptase inhibitor Nevirapine (Sigma SML0097) at 16 hpi, then harvested at 48 hpi. Cells were washed once with PBS prior to lysis with Trizol for RNA extraction or Laemmli buffer for Western blot analysis.

Western blots

Harvested and PBS washed cells were lysed in Lamalli buffer and kept at -20°C until ready for analysis. Prior to electrophoresis, cell lysates were sonicated till homogenous, denatured at 95°C 15mins, separated on 4-20% or 8-16% gradient Tris-

24

547   Glycine SDS polyacrylamide gels (Invitrogen), then transferred to a nitrocellulose

548   membrane. Membranes were blocked in 5% milk in PBS + 0.1% Tween (PBST+milk) and

549   stained with primary and secondary antibodies diluted 1:5000 in PBST+milk for 1hr to

550   over night. Signals were visualized by chemiluminescence with 2.5mM Luminol, 0.4mM

551   p-Coumaric acid, 0.1M Tris-HCl pH8.5 in dH$_2$O, supplemented with 0.0192% hydrogen

552   peroxide added prior to imaging.

553

554   **RNA quantification by qRT-PCR**

555   Done as previously described [44]. 1µg per sample of Trizol extracted RNA were

556   treated with 0.15µl/reaction of DNase I (NEB) and 1µl 10x DNase buffer in a 10µl reaction

557   for 30mins at 37 °C, followed by adding 5µl of 15mM EDTA and inactivating at 75 °C

558   10mins. 5µl of DNase treated RNA was then used for reverse transcription (RT) with Super

559   Script III (invitrogen) and random hexamer primers following manufacturer instructions in

560   a 20µl reaction at 50°C 1hr followed by 15mins inactivation at 70°C. Each 20µl RT

561   reaction was diluted with dH$_2$O to a final 120µl. qPCR was performed with 6µl diluted RT

562   product, 8µl 2x Power SYBR Green Master Mix (ABI), and 1µl each of 1mM forward and

563   reverse qPCR primer in a 16µl reaction. qPCR readouts were normalized to GAPDH levels

564   using the delta-delta Ct (ΔΔCt) method. All PCR primers used are listed in Supplemental

565   Table 1.

566

567   **RNA decay assay**

568   RNA stability were measured using the transcription stop method as previously

569   described [44]. Single cycle infected cells were treated at 2 days post infection with 5µg/ml

25

570   Actinomycin D (Sigma A9415), and harvested 0, 2.5, 5, and 7.5 hrs later. Viral RNA levels

571   at each time point were then assayed by qRT-PCR, calculated as fold change over time 0.

572   Statistical analysis of the rate of RNA decay was done on the $\log_2$ transformation of each

573   fold change value, using the R suite in the Rstudio interface, comparing slopes of linear

574   regression lines by analysis of covariance (ANCOVA) with the aov function using the

575   following code:

576   > DATATABLE <- read.csv("datafile.csv", header = TRUE)

577   > modv <- aov(val~type, data=DATATABLE)

578   > summary(modv)

579

580   **YTHDC1 PAR-CLIP**

581   PAR-CLIP was performed as before with minor modifications [20, 30]. For each

582   immunoprecipitation, 7x 15cm plates of 293T cells were seeded at 5 million cells/plate.

583   The next day, 5 plates were transfected with 19μg/plate of pNL4-3 for virus production,

584   the other 2 plates with (per plate) 2.5μg of pCMV-CD4, 10μg of pBC-CXCR4 and 7.5μg

585   of plasmids expressing either FLAG-GFP or FLAG-YTHDC1, all transfections with PEI.

586   The next day, the virus production plate media was changed, the CD4/CXCR4/FLAG-

587   tagged gene of interest transfected plates were split 1 in 5 to a total of 10x 15cm plates of

588   infection target cells. 3 days post transfection, the supernatant of virus production cells

589   were spun 3000rpm 10mins and filtered through 0.45μm pore filters to remove floating

590   cell, diluted 2x with fresh DMEM, and used to infect the infection target plates, resulting

591   in 15ml media/virus mix per plate. 48hpi, 8ml of supernatant were removed from each

592   plate, and replaced with 10ml of fresh media supplemented with 4-thiouridine (4SU) to a

593   final concentration of 100μM. The next day, 16hrs post 4SU pulse, the supernatents were

594   replaced with 3ml/plate of ice cold PBS, and subject to 2500 x100μJ/cm2 of 365nm UV

595   irradiation twice. Cells were then washed twice with PBS, scrapped off plates, and frozen

596   at -80°C. PAR-CLIP was then performed using a FLAG antibody (M2, Sigma) as described

597   in a published protocol [45]. RIPA buffer (NaCl 150 mM, Nonidet P-40 1%, Sodium

598   deoxycholate   0.5%, SDS   0.1%, Tris-HCl pH 7.4 25 mM) was used in place of PAR-

599   CLIP lysis buffer to ensure sufficient release of nuclear proteins. After elution, the resulting

600   RNA was passed through Biorad Micro Bio-Spin Columns with Bio-Gel P-30 to remove

601   excess salts, then subject to Illumina sequencing library preparation using the Illumina

602   TruSeq Small RNA Library Prep Kit. Multiplex barcode indexes used were RPI21, 22 and

603   23 for samples GFP control, DC1 repeat 1 and DC1 repeat 2, respectively.

604   Sequencing was done on a HiSeq 2000 in 50bp single read mode at the Duke Center

605   for Genomic and Computational Biology core facility. Data analysis was done as

606   previously described [44]. Reads <15nt or with a fastq quality score < Q33, along with

607   sequencing adaptors were removed using the FASTX-toolkit v0.014 [46]. Past-filter reads

608   were then aligned to the human genome (hg19) using Bowtie, and the human non-aligning

609   reads then aligned to the HIV-1 NL4-3 sequence with a single copy LTR (U5 on the 5'

610   end, and U3-R on the 3' end), thus 551-9626 nt of GenBank AF324493.2.), allowing 1

611   mismatch. An in-house Perl script was used to only retain reads containing the T>C

612   conversions resulting from UV-crosslinked 4SU. Peak calling was done using PARalyzer

613   v1.1   [47]   (with   the   parameters:

614   BANDWIDTH=3   CONVERSION=T>C

615   MINIMUM_READ_COUNT_PER_GROUP=10

27

616   MINIMUM_READ_COUNT_PER_CLUSTER=1

617   MINIMUM_READ_COUNT_FOR_KDE=5   MINIMUM_CLUSTER_SIZE=15

618   MINIMUM_CONVERSION_LOCATIONS_FOR_CLUSTER=2

619   MINIMUM_CONVERSION_COUNT_FOR_CLUSTER=1

620   MINIMUM_READ_COUNT_FOR_CLUSTER_INCLUSION=1

621   MINIMUM_READ_LENGTH=10

622   MAXIMUM_NUMBER_OF_NON_CONVERSION_MISMATCHES=1

623   EXTEND_BY_READ). After file format conversions using SAMtools [48], all data was

624   visualized using Integrative Genomics Viewer (IGV) [49].

625

626   **Primer-ID RNA-seq splicing assay**

627   YTHDC1 knockdown or overexpressing 293T cells treated and infected as

628   mentioned above were performed in 6 well plates, 2 wells per sample were collected and

629   the RNA extracted with Trizol (Invitrogen). The samples were subsequently amplified and

630   sequenced as previously described [31].

631

632   **PA-m⁶A-seq**

633   Done as previously [20, 39]. Briefly, 270 million each of wildtype and +ALKBH5

634   CEM cells were used, each infected with HIV-1 produced from ten 15cm plates of 293T

635   cells and pulsed with 100μM of 4SU one day prior to harvest. Total RNA extracted with

636   Trizol and poly(A) purified using the Poly(A)Purist MAG Kit (Invitrogen #AM1922).

637   After m⁶A immunoprecipitation, Illumina sequencing libraries were prepared using the

638   NEBNext small RNA kit (E7300S), using multiplex barcode indexes RPI5 and 6 for

639   control and +ALKBH5 samples, and sequenced on an Illumina Novaseq 6000 sequencer.

640   Data analysis done as mentioned above for PAR-CLIP.

641

642   **Quantification and statistical analysis**

643   All statistical details are listed in the figure legends. All averaged data include error

644   bars that denote standard deviation. All statistical analysis done by Student's T-test

645   comparing subjects to control, with the exception of RNA decay studies, where the slopes

646   of regression lines were compared by ANCOVA.

647

648   **Data availability**

649   Deep sequencing data for the YTHDC1 PAR-CLIP have been deposited at the

650   NCBI GEO database under accession number GSE165473, while the splicing analysis data

651   is under accession number GSE166237.

652

653   **Acknowledgements**

654   The following reagents were obtained through the NIH AIDS Reagent Program,

655   Division of AIDS, NIAID, NIH: HIV-1 p24 Gag Monoclonal (#24-3) from Michael Malim

656   and HIV-1 NL4-3 Infectious Molecular Clone (pNL4-3, #114) Malcolm Martin. We thank

657   Ananda Ayyappan Jaguva Vasudevan for cloning assistance, as well as the labs of

658   Christopher Holley, Nicholas Heaton, Dennis Ko and Qi-Jing Li for allowing us to use

659   their equipment.

660

661

662 **References**

663 1.   Dominissini D, Moshitch-Moshkovitz S, Schwartz S, Salmon-Divon M, Ungar L,

664 Osenberg S, et al. Topology of the human and mouse m6A RNA methylomes revealed

665 by m6A-seq. Nature. 2012;485(7397):201-6. Epub 2012/05/12. doi:

666 10.1038/nature11112. PubMed PMID: 22575960.

667 2.   Meyer KD, Saletore Y, Zumbo P, Elemento O, Mason CE, Jaffrey SR.

668 Comprehensive analysis of mRNA methylation reveals enrichment in 3' UTRs and

669 near stop codons. Cell. 2012;149(7):1635-46. Epub 2012/05/23. doi:

670 10.1016/j.cell.2012.05.003. PubMed PMID: 22608085; PubMed Central PMCID:

671 PMCPMC3383396.

672 3.   Bokar JA, Shambaugh ME, Polayes D, Matera AG, Rottman FM. Purification

673 and cDNA cloning of the AdoMet-binding subunit of the human mRNA (N6-

674 adenosine)-methyltransferase. Rna. 1997;3(11):1233-47. Epub 1997/12/31.

675 PubMed PMID: 9409616; PubMed Central PMCID: PMCPMC1369564.

676 4.   Ping XL, Sun BF, Wang L, Xiao W, Yang X, Wang WJ, et al. Mammalian WTAP is

677 a regulatory subunit of the RNA N6-methyladenosine methyltransferase. Cell Res.

678 2014;24(2):177-89. Epub 2014/01/11. doi: 10.1038/cr.2014.3. PubMed PMID:

679 24407421; PubMed Central PMCID: PMCPMC3915904.

680 5.   Liu J, Yue Y, Han D, Wang X, Fu Y, Zhang L, et al. A METTL3-METTL14

681 complex mediates mammalian nuclear RNA N6-adenosine methylation. Nat Chem

682 Biol. 2014;10(2):93-5. Epub 2013/12/10. doi: 10.1038/nchembio.1432. PubMed

683 PMID: 24316715; PubMed Central PMCID: PMCPMC3911877.

684   6.   Shi H, Wei J, He C. Where, When, and How: Context-Dependent Functions of

685   RNA Methylation Writers, Readers, and Erasers. Molecular cell. 2019;74(4):640-50.

686   Epub 2019/05/18. doi: 10.1016/j.molcel.2019.04.025. PubMed PMID: 31100245;

687   PubMed Central PMCID: PMCPMC6527355.

688   7.   Zheng G, Dahl JA, Niu Y, Fedorcsak P, Huang CM, Li CJ, et al. ALKBH5 is a

689   mammalian RNA demethylase that impacts RNA metabolism and mouse fertility.

690   Molecular cell. 2013;49(1):18-29. Epub 2012/11/28. doi:

691   10.1016/j.molcel.2012.10.015. PubMed PMID: 23177736; PubMed Central PMCID:

692   PMCPMC3646334.

693   8.   Jia G, Fu Y, Zhao X, Dai Q, Zheng G, Yang Y, et al. N6-methyladenosine in

694   nuclear RNA is a major substrate of the obesity-associated FTO. Nat Chem Biol.

695   2011;7(12):885-7. Epub 2011/10/18. doi: 10.1038/nchembio.687. PubMed PMID:

696   22002720; PubMed Central PMCID: PMCPMC3218240.

697   9.   Wang X, Lu Z, Gomez A, Hon GC, Yue Y, Han D, et al. N6-methyladenosine-

698   dependent regulation of messenger RNA stability. Nature. 2014;505(7481):117-20.

699   Epub 2013/11/29. doi: 10.1038/nature12730. PubMed PMID: 24284625; PubMed

700   Central PMCID: PMCPMC3877715.

701   10.   Xiao W, Adhikari S, Dahal U, Chen YS, Hao YJ, Sun BF, et al. Nuclear m(6)A

702   Reader YTHDC1 Regulates mRNA Splicing. Molecular cell. 2016;61(4):507-19. Epub

703   2016/02/16. doi: 10.1016/j.molcel.2016.01.012. PubMed PMID: 26876937.

704   11.   Wang X, Zhao BS, Roundtree IA, Lu Z, Han D, Ma H, et al. N(6)-

705   methyladenosine Modulates Messenger RNA Translation Efficiency. Cell.

706   2015;161(6):1388-99. Epub 2015/06/06. doi: 10.1016/j.cell.2015.05.014. PubMed

707   PMID: 26046440; PubMed Central PMCID: PMCPMC4825696.

708   12.   Roundtree IA, Luo GZ, Zhang Z, Wang X, Zhou T, Cui Y, et al. YTHDC1

709   mediates nuclear export of N(6)-methyladenosine methylated mRNAs. eLife. 2017;6.

710   Epub 2017/10/07. doi: 10.7554/eLife.31311. PubMed PMID: 28984244; PubMed

711   Central PMCID: PMCPMC5648532.

712   13.   Zaccara S, Jaffrey SR. A Unified Model for the Function of YTHDF Proteins in

713   Regulating m(6)A-Modified mRNA. Cell. 2020;181(7):1582-95 e18. Epub

714   2020/06/04. doi: 10.1016/j.cell.2020.05.012. PubMed PMID: 32492408; PubMed

715   Central PMCID: PMCPMC7508256.

716   14.   Lasman L, Krupalnik V, Viukov S, Mor N, Aguilera-Castrejon A, Schneir D, et

717   al. Context-dependent functional compensation between Ythdf m(6)A reader

718   proteins. Genes & development. 2020;34(19-20):1373-91. Epub 2020/09/19. doi:

719   10.1101/gad.340695.120. PubMed PMID: 32943573; PubMed Central PMCID:

720   PMCPMC7528697.

721   15.   Courtney DG, Chalem A, Bogerd HP, Law BA, Kennedy EM, Holley CL, et al.

722   Extensive Epitranscriptomic Methylation of A and C Residues on Murine Leukemia

723   Virus Transcripts Enhances Viral Gene Expression. mBio. 2019;10(3):e01209-19.

724   Epub 2019/06/13. doi: 10.1128/mBio.01209-19. PubMed PMID: 31186331;

725   PubMed Central PMCID: PMCPMC6561033.

726   16.   Tsai K, Cullen BR. Epigenetic and epitranscriptomic regulation of viral

727   replication. Nat Rev Microbiol. 2020;18(10):559-70. Epub 2020/06/14. doi:

728   10.1038/s41579-020-0382-3. PubMed PMID: 32533130; PubMed Central PMCID:

729   PMCPMC7291935.

730   17.   Tirumuru N, Zhao BS, Lu W, Lu Z, He C, Wu L. N(6)-methyladenosine of HIV-1

731   RNA regulates viral infection and HIV-1 Gag protein expression. eLife.

732   2016;5:e15528. doi: 10.7554/eLife.15528. PubMed PMID: 27371828; PubMed

733   Central PMCID: PMC4961459.

734   18.   Lichinchi G, Gao S, Saletore Y, Gonzalez GM, Bansal V, Wang Y, et al. Dynamics

735   of the human and viral m(6)A RNA methylomes during HIV-1 infection of T cells.

736   Nature microbiology. 2016;1:16011. doi: 10.1038/nmicrobiol.2016.11. PubMed

737   PMID: 27572442; PubMed Central PMCID: PMC6053355.

738   19.   Courtney DG, Tsai K, Bogerd HP, Kennedy EM, Law BA, Emery A, et al.

739   Epitranscriptomic Addition of m5C to HIV-1 Transcripts Regulates Viral Gene

740   Expression. Cell host & microbe. 2019;26(2):217-27.e6. doi:

741   10.1016/j.chom.2019.07.005. PubMed PMID: 31415754; PubMed Central PMCID:

742   PMCPMC6714563.

743   20.   Kennedy EM, Bogerd HP, Kornepati AV, Kang D, Ghoshal D, Marshall JB, et al.

744   Posttranscriptional m(6)A Editing of HIV-1 mRNAs Enhances Viral Gene Expression.

745   Cell host & microbe. 2016;19(5):675-85. doi: 10.1016/j.chom.2016.04.002. PubMed

746   PMID: 27117054; PubMed Central PMCID: PMC4867121.

747   21.   Chu CC, Liu B, Plangger R, Kreutz C, Al-Hashimi HM. m6A minimally impacts

748   the structure, dynamics, and Rev ARM binding properties of HIV-1 RRE stem IIB.

749   PloS one. 2019;14(12):e0224850. Epub 2019/12/12. doi:

750   10.1371/journal.pone.0224850. PubMed PMID: 31825959; PubMed Central PMCID:

33

751   PMCPMC6905585 based drug discovery company. This does not alter our adherence

752   to PLOS ONE policies on sharing data and materials.

753   22.   Lu W, Tirumuru N, St Gelais C, Koneru PC, Liu C, Kvaratskhelia M, et al. N(6)-

754   Methyladenosine-binding proteins suppress HIV-1 infectivity and viral production.

755   The Journal of biological chemistry. 2018;293(34):12992-3005. Epub 2018/07/07.

756   doi: 10.1074/jbc.RA118.004215. PubMed PMID: 29976753; PubMed Central PMCID:

757   PMCPMC6109920.

758   23.   Jurczyszak D, Zhang W, Terry SN, Kehrer T, Bermudez Gonzalez MC,

759   McGregor E, et al. HIV protease cleaves the antiviral m6A reader protein YTHDF3 in

760   the viral particle. PLoS pathogens. 2020;16(2):e1008305. Epub 2020/02/14. doi:

761   10.1371/journal.ppat.1008305. PubMed PMID: 32053707; PubMed Central PMCID:

762   PMCPMC7043784.

763   24.   Lu M, Zhang Z, Xue M, Zhao BS, Harder O, Li A, et al. N(6)-methyladenosine

764   modification enables viral RNA to escape recognition by RNA sensor RIG-I. Nature

765   microbiology. 2020. Epub 2020/02/06. doi: 10.1038/s41564-019-0653-9. PubMed

766   PMID: 32015498.

767   25.   Bogerd HP, Doehle BP, Wiegand HL, Cullen BR. A single amino acid difference

768   in the host APOBEC3G protein controls the primate species specificity of HIV type 1

769   virion infectivity factor. Proceedings of the National Academy of Sciences of the

770   United States of America. 2004;101(11):3770-4. Epub 2004/03/05. doi:

771   10.1073/pnas.0307713101. PubMed PMID: 14999100; PubMed Central PMCID:

772   PMCPMC374319.

34

773   26.   Mangeat B, Turelli P, Liao S, Trono D. A single amino acid determinant

774   governs the species-specific sensitivity of APOBEC3G to Vif action. The Journal of

775   biological chemistry. 2004;279(15):14481-3. Epub 2004/02/18. doi:

776   10.1074/jbc.C400060200. PubMed PMID: 14966139.

777   27.   Schrofelbauer B, Chen D, Landau NR. A single amino acid of APOBEC3G

778   controls its species-specific interaction with virion infectivity factor (Vif).

779   Proceedings of the National Academy of Sciences of the United States of America.

780   2004;101(11):3927-32. Epub 2004/02/24. doi: 10.1073/pnas.0307132101.

781   PubMed PMID: 14978281; PubMed Central PMCID: PMCPMC374346.

782   28.   Cullen BR, Greene WC. Functions of the auxiliary gene products of the human

783   immunodeficiency virus type 1. Virology. 1990;178(1):1-5. Epub 1990/09/01. doi:

784   10.1016/0042-6822(90)90373-y. PubMed PMID: 2202146.

785   29.   Stoltzfus CM. Chapter 1. Regulation of HIV-1 alternative RNA splicing and its

786   role in virus replication. Adv Virus Res. 2009;74:1-40. Epub 2009/08/25. doi:

787   10.1016/S0065-3527(09)74001-1. PubMed PMID: 19698894.

788   30.   Hafner M, Landthaler M, Burger L, Khorshid M, Hausser J, Berninger P, et al.

789   Transcriptome-wide identification of RNA-binding protein and microRNA target

790   sites by PAR-CLIP. Cell. 2010;141(1):129-41. doi: 10.1016/j.cell.2010.03.009.

791   PubMed PMID: 20371350; PubMed Central PMCID: PMC2861495.

792   31.   Emery A, Zhou S, Pollom E, Swanstrom R. Characterizing HIV-1 Splicing by

793   Using Next-Generation Sequencing. Journal of virology. 2017;91(6). Epub

794   2017/01/13. doi: 10.1128/JVI.02515-16. PubMed PMID: 28077653; PubMed

795   Central PMCID: PMCPMC5331825.

796   32.   Park OH, Ha H, Lee Y, Boo SH, Kwon DH, Song HK, et al. Endoribonucleolytic

797   Cleavage of m(6)A-Containing RNAs by RNase P/MRP Complex. Molecular cell.

798   2019;74(3):494-507 e8. Epub 2019/04/02. doi: 10.1016/j.molcel.2019.02.034.

799   PubMed PMID: 30930054.

800   33.   Meyer KD, Jaffrey SR. The dynamic epitranscriptome: N6-methyladenosine

801   and gene expression control. Nature reviews Molecular cell biology.

802   2014;15(5):313-26. doi: 10.1038/nrm3785. PubMed PMID: 24713629; PubMed

803   Central PMCID: PMC4393108.

804   34.   Fry NJ, Law BA, Ilkayeva OR, Holley CL, Mansfield KD. N(6)-methyladenosine

805   is required for the hypoxic stabilization of specific mRNAs. Rna. 2017;23(9):1444-

806   55. Epub 2017/06/15. doi: 10.1261/rna.061044.117. PubMed PMID: 28611253;

807   PubMed Central PMCID: PMCPMC5558913.

808   35.   Price AM, Hayer KE, McIntyre ABR, Gokhale NS, Abebe JS, Della Fera AN, et al.

809   Direct RNA sequencing reveals m(6)A modifications on adenovirus RNA are

810   necessary for efficient splicing. Nature communications. 2020;11(1):6016. Epub

811   2020/11/28. doi: 10.1038/s41467-020-19787-6. PubMed PMID: 33243990;

812   PubMed Central PMCID: PMCPMC7691994.

813   36.   Alarcon CR, Goodarzi H, Lee H, Liu X, Tavazoie S, Tavazoie SF. HNRNPA2B1 Is

814   a Mediator of m(6)A-Dependent Nuclear RNA Processing Events. Cell.

815   2015;162(6):1299-308. Epub 2015/09/01. doi: 10.1016/j.cell.2015.08.011. PubMed

816   PMID: 26321680; PubMed Central PMCID: PMCPMC4673968.

817   37.   Bartosovic M, Molares HC, Gregorova P, Hrossova D, Kudla G, Vanacova S. N6-

818   methyladenosine demethylase FTO targets pre-mRNAs and regulates alternative

819   splicing and 3'-end processing. Nucleic acids research. 2017;45(19):11356-70. Epub

820   2017/10/05. doi: 10.1093/nar/gkx778. PubMed PMID: 28977517; PubMed Central

821   PMCID: PMCPMC5737695.

822   38.   Purcell DF, Martin MA. Alternative splicing of human immunodeficiency virus

823   type 1 mRNA modulates viral protein expression, replication, and infectivity. Journal

824   of virology. 1993;67(11):6365-78. Epub 1993/11/01. doi: 10.1128/JVI.67.11.6365-

825   6378.1993. PubMed PMID: 8411338; PubMed Central PMCID: PMCPMC238071.

826   39.   Tsai K, Courtney DG, Cullen BR. Addition of m6A to SV40 late mRNAs

827   enhances viral structural gene expression and replication. PLoS pathogens.

828   2018;14(2):e1006919. doi: 10.1371/journal.ppat.1006919. PubMed PMID:

829   29447282; PubMed Central PMCID: PMC5831754.

830   40.   Cullen BR. Nuclear mRNA export: insights from virology. Trends in

831   biochemical sciences. 2003;28(8):419-24. Epub 2003/08/23. doi: 10.1016/S0968-

832   0004(03)00142-7. PubMed PMID: 12932730.

833   41.   Tazi J, Bakkour N, Marchand V, Ayadi L, Aboufirassi A, Branlant C. Alternative

834   splicing: regulation of HIV-1 multiplication as a target for therapeutic action. FEBS J.

835   2010;277(4):867-76. Epub 2010/01/20. doi: 10.1111/j.1742-4658.2009.07522.x.

836   PubMed PMID: 20082634.

837   42.   Adachi A, Gendelman HE, Koenig S, Folks T, Willey R, Rabson A, et al.

838   Production of acquired immunodeficiency syndrome-associated retrovirus in

839   human and nonhuman cells transfected with an infectious molecular clone. J Virol.

840   1986;59(2):284-91. Epub 1986/08/01. PubMed PMID: 3016298; PubMed Central

841   PMCID: PMC253077.

842   43.   Mefferd AL, Bogerd HP, Irwan ID, Cullen BR. Insights into the mechanisms

843   underlying the inactivation of HIV-1 proviruses by CRISPR/Cas. Virology.

844   2018;520:116-26. Epub 2018/06/02. doi: 10.1016/j.virol.2018.05.016. PubMed

845   PMID: 29857168; PubMed Central PMCID: PMCPMC6100742.

846   44.   Tsai K, Jaguva Vasudevan AA, Martinez Campos C, Emery A, Swanstrom R,

847   Cullen BR. Acetylation of Cytidine Residues Boosts HIV-1 Gene Expression by

848   Increasing Viral RNA Stability. Cell host & microbe. 2020;28(2):306-12 e6. Epub

849   2020/06/14. doi: 10.1016/j.chom.2020.05.011. PubMed PMID: 32533923; PubMed

850   Central PMCID: PMCPMC7429276.

851   45.   Spitzer J, Hafner M, Landthaler M, Ascano M, Farazi T, Wardle G, et al. PAR-

852   CLIP (Photoactivatable Ribonucleoside-Enhanced Crosslinking and

853   Immunoprecipitation): a step-by-step protocol to the transcriptome-wide

854   identification of binding sites of RNA-binding proteins. Methods in enzymology.

855   2014;539:113-61. Epub 2014/03/04. doi: 10.1016/B978-0-12-420120-0.00008-6.

856   PubMed PMID: 24581442; PubMed Central PMCID: PMCPMC4180672.

857   46.   Gordon A, Hannon G. FastX Toolkit

858   http://hannonlab.cshl.edu/fastx_toolkit/2010. Available from:

859   http://hannonlab.cshl.edu/fastx_toolkit/.

860   47.   Corcoran DL, Georgiev S, Mukherjee N, Gottwein E, Skalsky RL, Keene JD, et

861   al. PARalyzer: definition of RNA binding sites from PAR-CLIP short-read sequence

862   data. Genome Biol. 2011;12(8):R79. Epub 2011/08/20. doi: 10.1186/gb-2011-12-8-

863   r79. PubMed PMID: 21851591; PubMed Central PMCID: PMC3302668.

864   48.   Li H, Handsaker B, Wysoker A, Fennell T, Ruan J, Homer N, et al. The

865   Sequence Alignment/Map format and SAMtools. Bioinformatics. 2009;25(16):2078-

866   9. Epub 2009/06/10. doi: 10.1093/bioinformatics/btp352. PubMed PMID:

867   19505943; PubMed Central PMCID: PMCPMC2723002.

868   49.   Robinson JT, Thorvaldsdottir H, Winckler W, Guttman M, Lander ES, Getz G,

869   et al. Integrative genomics viewer. Nat Biotechnol. 2011;29(1):24-6. Epub

870   2011/01/12. doi: 10.1038/nbt.1754. PubMed PMID: 21221095; PubMed Central

871   PMCID: PMCPMC3346182.

872

873

874   **Figures**

875

876
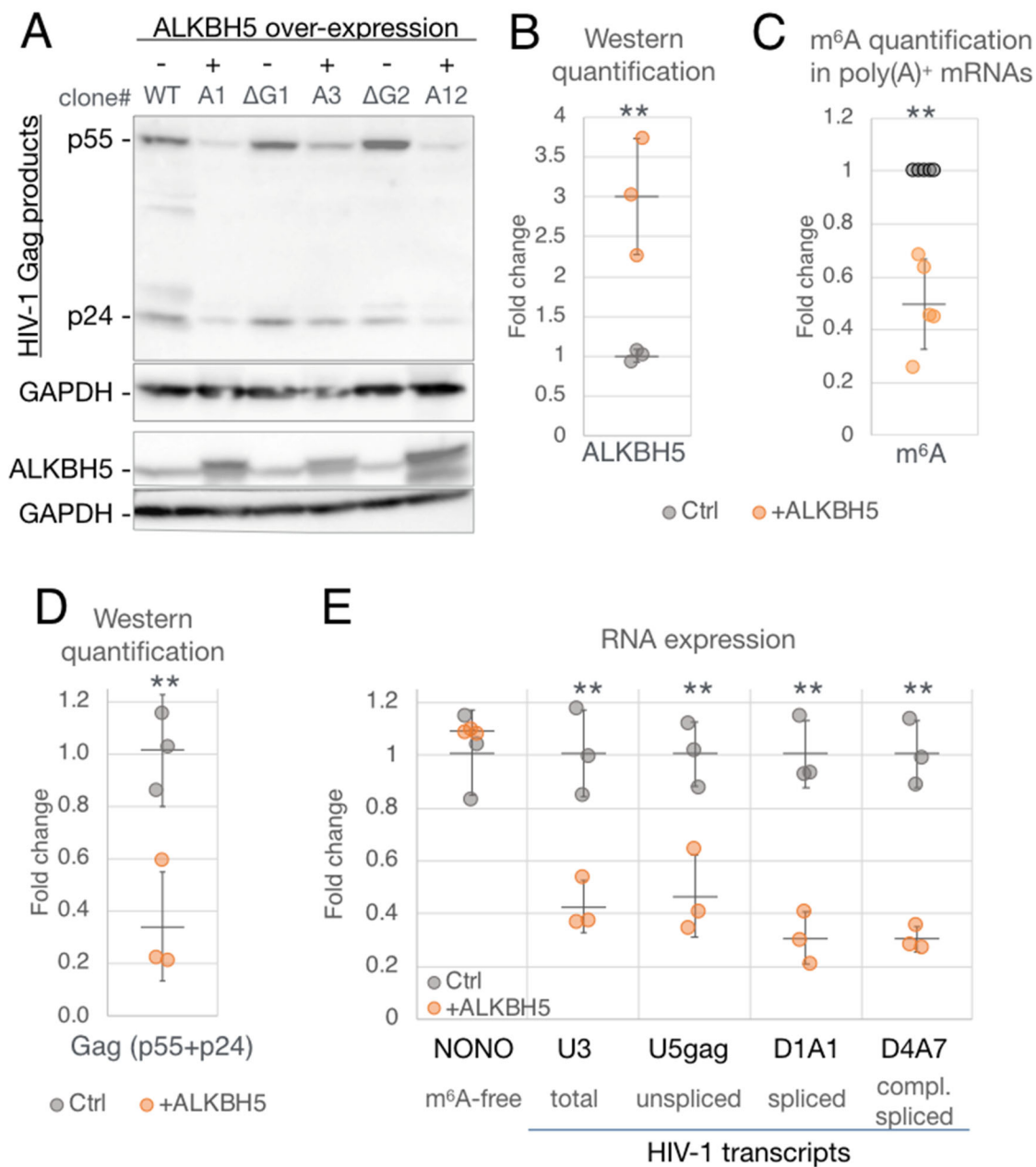
877   **Fig 1. Global depletion of m^6A in T cells suppresses HIV-1 RNA and protein**

878   **expression.** Three separate clones of the CD4$^+$ CEM T cell line (A1, A3 and A12) were

879   obtained by transduction with a lentiviral ALKBH5 expression vector (+ALKBH5). They

880   were then compared to WT CEM cells (Ctrl) for the level of m^6A present on poly(A)$^+$

40

881   RNAs. (A) HIV-1 Gag expression levels were analyzed by Western blot at 2 dpi after single

882   cycle HIV-1 infection of +ALKBH5 CEM cells or control cells (one WT and the others

883   expressing the irrelevant GFP-targeted Cas9 (ΔG)). Also analyzed were ALKBH5 (the

884   overexpressed ALKBH5 is epitope tagged and runs slightly slower than endogenous

885   ALKBH5) and GAPDH, as a loading control. (B) ALKBH5 band intensities from panel A

886   were quantified and are given relative to control cells, set at 1. (C) The m^6A content of

887   poly(A)$^+$ mRNAs from Ctrl and +ALKBH5 cells was quantified by ELISA and is given

888   relative to control cells, set at 1 (n=5). (D) Quantification of the HIV-1 Gag band intensities

889   (p24 + p55) from panel A. (E) Aliquotes of the samples from panel C were analyzed for

890   viral RNA expression levels by qRT-PCR, with primers targeting different viral transcripts

891   as marked. The m^6A-free cellular transcript (NONO) served as a negative control.

892   Statistical analyses by two-tailed Student's T test, error bars=SD, *$p<0.05$, **$p<0.01$.

893
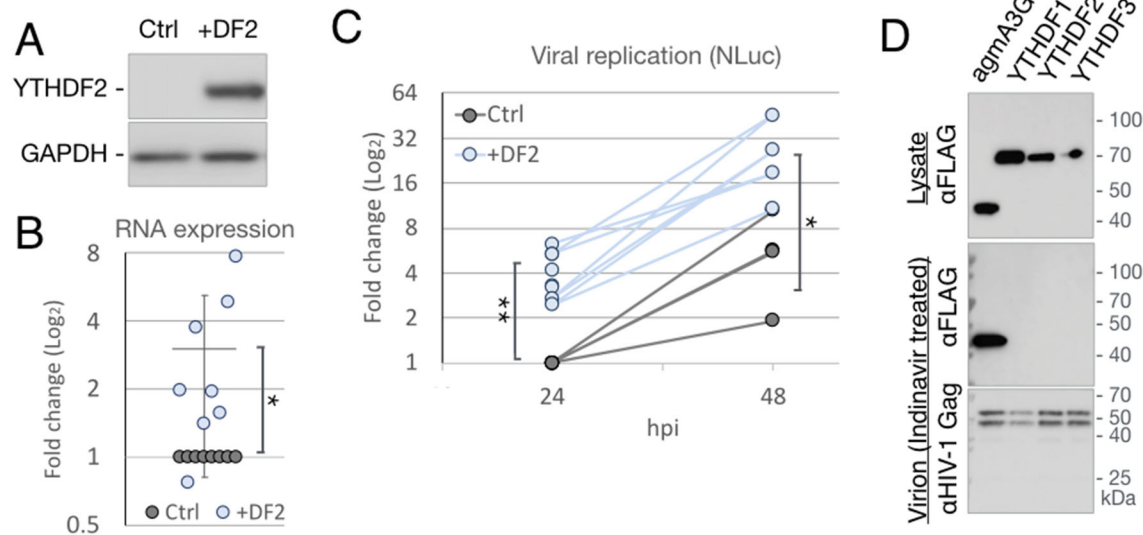
Fig 2. The cytosolic m⁶A reader YTHDF2 enhances HIV-1 replication yet is not packaged into virions. (A-C) 293T cells transfected with either empty vector (Ctrl) or a YTHDF2 expression plasmid (+DF2) were infected with the NL4-3-NLuc reporter virus and collected at 24 hpi for (A) Western blot detection of over-expressed YTHDF2 or (B) qRT-PCR analysis of viral RNA expression, n=8. (C) Quantification of the virally encoded NLuc protein as a measure of viral replication at 24 hpi (n=8) and 48 hpi (n=4). (D) 293T cells were co-transfected with NL4-3-NLuc along with expression vectors expressing FLAG-tagged YTHDF readers or agmA3G and treated with the HIV-1 protease inhibitor indinavir. Lysates of the virus producer cells (upper panel) and purified virions from the supernatant media (two lower panels) were analyzed by Western blot for presence of the FLAG-tagged YTHDF or agmA3G protein and the HIV-1 Gag protein. Statistical analysis by two-tailed Student's T test, *p<0.05, **p<0.01, error bars=SD.

908
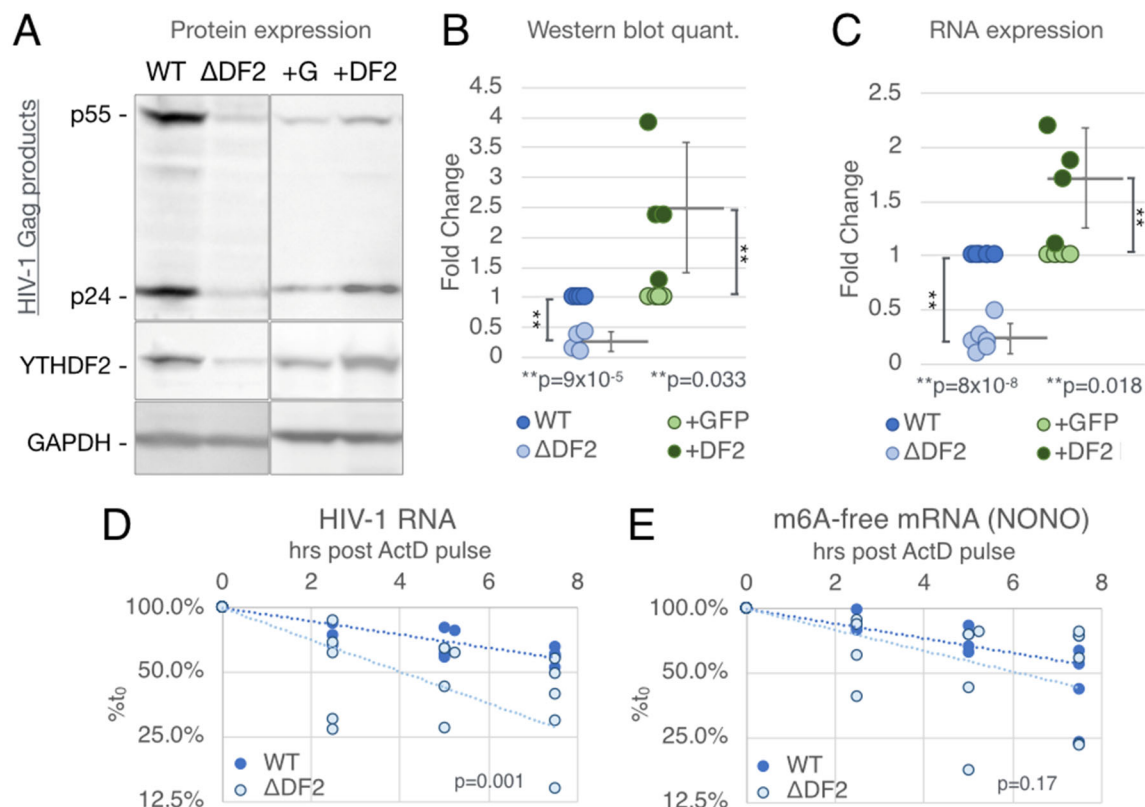
Fig 3. The cytosolic m^{6}A reader YTHDF2 enhances HIV-1 RNA stability in CD4$^+$ T

cells. YTHDF2 knock out CD4$^+$ T cells (ΔDF2), WT control cells (WT), and cells

transduced with a lentiviral YTHDF2 or GFP expression vector (+DF2 or +G) were used

for the following single cycle infection assays. (A) Viral Gag protein expression levels

analyzed by Western blot. (B) Quantification of protein band intensities of Western blots

as shown in panel A (n=4) (C) Viral RNA expression assayed by qRT-PCR (WT &

ΔYTHDF2 n=6, +GFP & +YTHDF2 n=5). (D-E) Viral RNA stability assayed by treating

infected WT or ΔDF2 cells at 2 dpi with ActD and collecting RNA at the indicated time

points. (D) Viral RNA levels analyzed by qRT-PCR and shown as % of the RNA level at

time point 0. (E) RNA stability of a m^{6}A-free host transcript (NONO) assayed as a control.

Statistical analysis of data in B and C used the two-tailed Student's T test, p values as

43

920   marked, error bars=SD. For panels F and G, slopes of regression lines were compared by

921   ANCOVA, n=5.

922

923

45
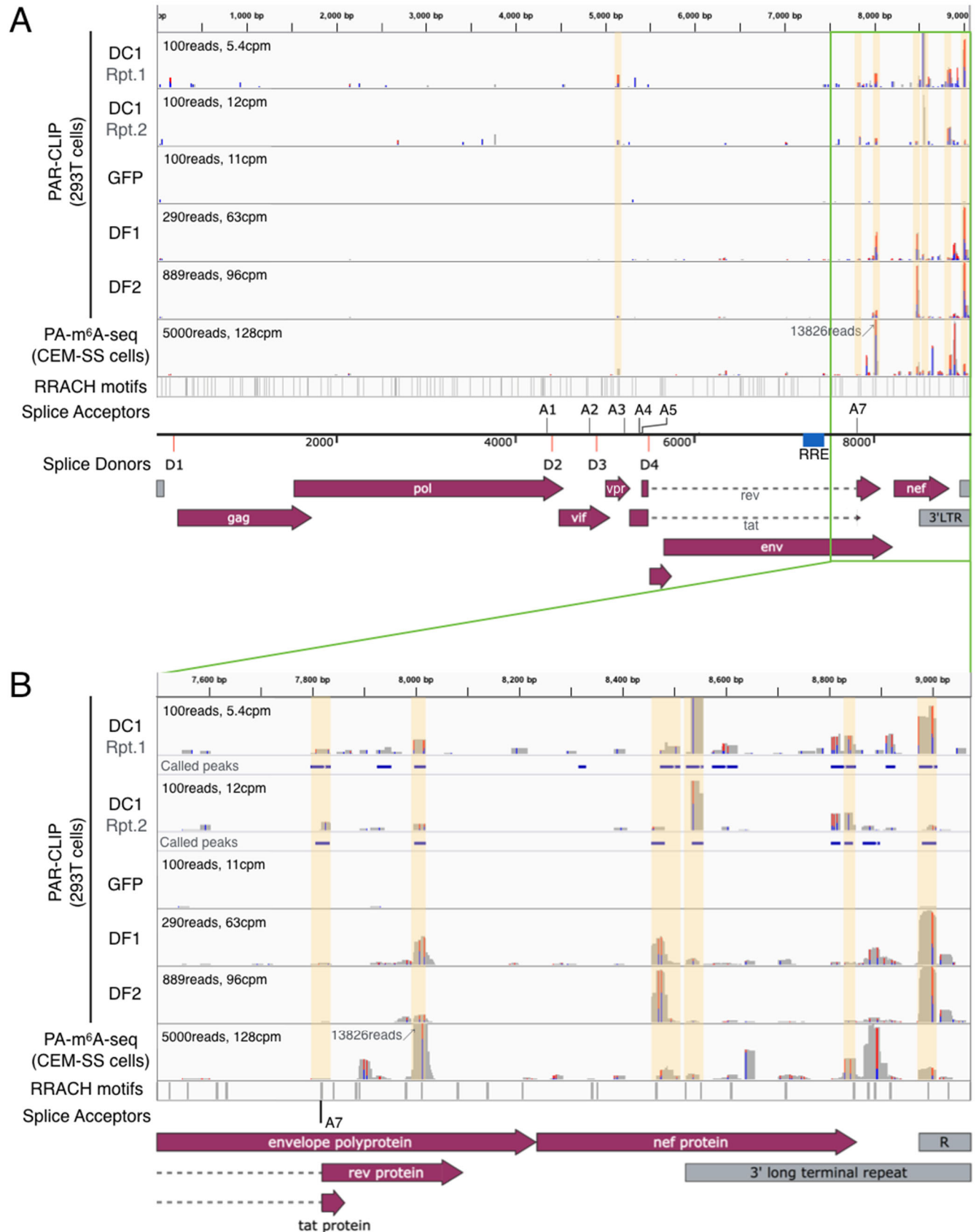
924 **Fig 4. The nuclaer m⁶A reader YTHDC1 binds HIV-1 RNA at previously mapped**

925 **m⁶A sites.** PAR-CLIP was performed on 293T cells transfected with FLAG-GFP or

926 FLAG-YTHDC1, and infected with HIV-1, by immunoprecipitating protein-RNA

927 complexes using a FLAG antibody. Sequencing reads were mapped to the HIV-1 genome,

928 with two independent repeats of YTHDC1 PAR-CLIP (DC1 lanes) shown alongside

929 previously published YTHDF1 & YTHDF2 PAR-CLIP (DF1 & DF2 lanes) and m⁶A

930 mapping results (PA-m⁶A-seq lane) [19, 20]. An overview of the whole HIV-1 genome is

931 shown in (A), with the 3'end (3' of 7,500bp) shown in (B) where the major m⁶A sites are

932 located. Locations of the m⁶A motif 5'-RRACH-3' are shown in the bottom lane, with a

933 diagram of the splice donors and acceptors relative to the HIV-1 genome map shown

934 beneath. Significant YTHDC1 peaks called by PARalyzer shown as blue bars beneath each

935 DC1 lane in (B). PARalyzer-called peaks that overlap with m⁶A sites and 5'-RRACH-3'

936 motifs are highlighted in yellow.

937

46
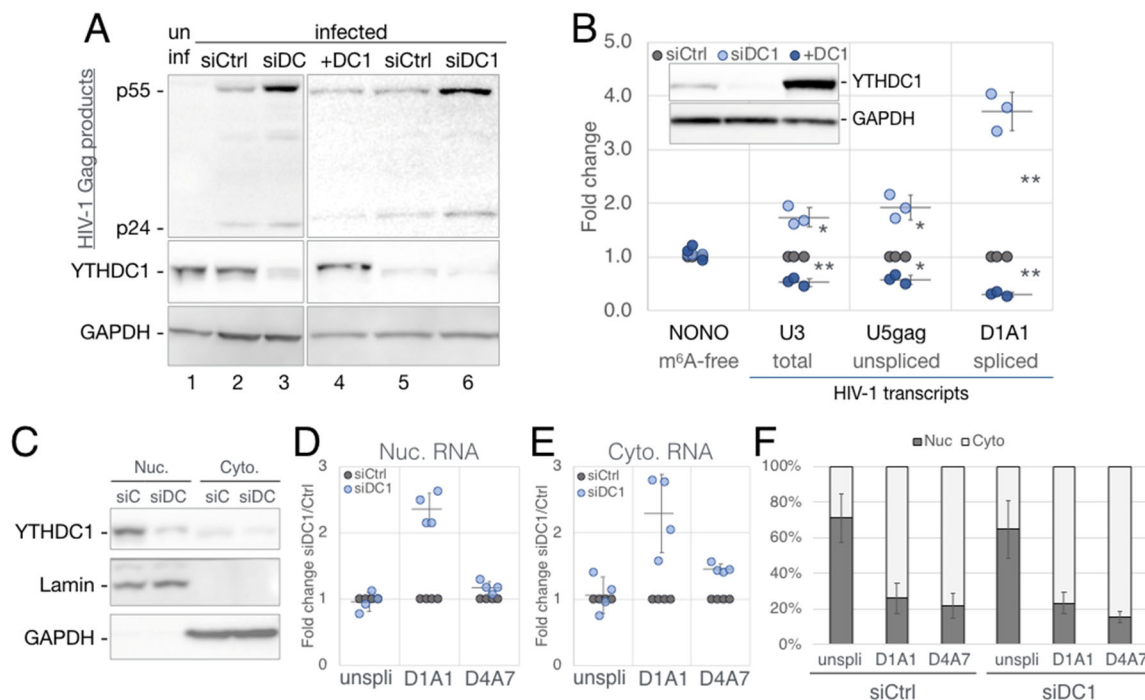
Fig 5. YTHDC1 regulates HIV-1 gene expression with no detectable effect on RNA nuclear export. 293T cells transfected with non-targeting (siCtrl, gray) or YTHDC1-targeting (siDC1, light blue) siRNAs were co-transfected with a YTHDC1 expression vector (+DC1, dark blue) or empty vector. HIV-1 single cycle infections were performed for the following analyses: (A) Viral Gag protein expression assayed by Western blot, co-stained with a YTHDC1 antibody. (B) Viral RNA levels assayed by qRT-PCR, n=3, with the m^6A-free host NONO mRNA as a control. A representative Western blot shown in the top left inset depicts the validation of YTHDC1 levels for the samples used in this panel. (C-F) Subcellular fractionation assay of infected siCtrl and siDC1 cells. (C) Western blot validation of fractionation, stained for YTHDC1, nuclear Lamin A/C, and the cytosolic protein GAPDH. (D-F) HIV-1 transcript alternative splice forms were quantified by qRT-PCR with primers targeting unspliced (unspli, U5-gag), and the D1/A1, and D4/A7 splice junctions, calculated as fold change of siDC1 over siCtrl in the nuclear (D), and cytosolic fraction (E). (F) The same RNA quantification as panels (D-E) calculated as percent

953   nuclear and percent cytoplasmic. Statistical analysis used Student's T test, error bars=SD,

954   *<0.05, **<0.01.

955
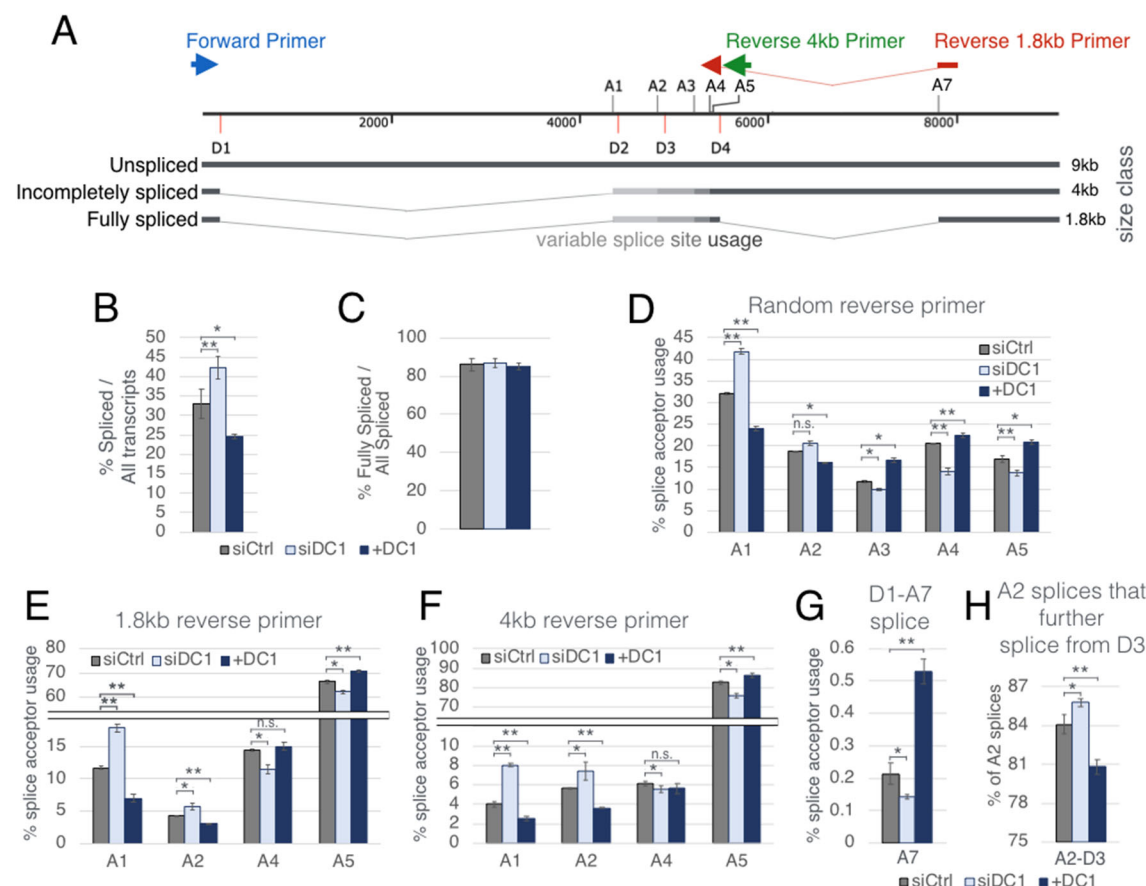
Fig 6. YTHDC1 regulates the relative expression of alternatively spliced HIV-1 RNAs.

Viral transcript spliced isoforms in infected siCtrl, siDC1, and +DC1 cells 48 hpi were analyzed by PrimerID RNA-seq, n=3 [31]. (A) Schematic of HIV-1 splice donors and acceptors relative to the three major classes of spliced viral RNAs. Top arrows depict the locations of primers used to amplify sequences for RNA-seq, including the common 5' forward primer in blue, the reverse 4kb primer in green, and the reverse 1.8kb primer in red spanning the D4/A7 splice junction. A random reverse primer was also used but is not shown. (B) Spliced transcripts are given as a percentage of all transcripts (1.8kb+4kb class read counts / total read counts). (C) Percent of fully spliced transcripts over all spliced transcripts (1.8kb / (1.8kb+4kb) read counts). (D-F) Splice acceptor usage assayed using the common forward primer in conjunction with the random reverse primer (D), 1.8kb

49

967   reverse primer (E) and 4kb reverse primer (F). Use of acceptor A3 results in long transcripts

968   that are biased against when amplifying using the 1.8 or 4kb reverse primers, A3 usage is

969   thus only shown with the random reverse primer. (G) Percent occurance of D1/A7 splices.

970   (H) Percent occurance of A2-utilizing spliced RNAs that subsequently splice from D3.

971   Statistical analysis used Student's T test, error bars=SD, *<0.05, **<0.01.

972   **Supplemental Material**

973
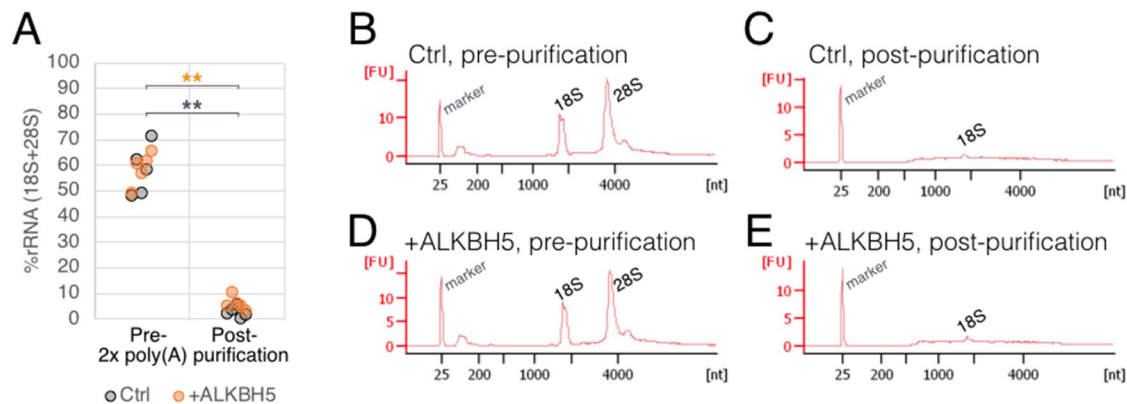
974   **Fig. S1. Validation of poly(A) purification for m^6A ELISA quantification.**

975   75ng each of pre-purification and post-purification RNA from WT CEM T cells (Ctrl) and

976   ALKBH5-overexpressing CEM T cells (+ALKBH5) were analyzed on an Agilent

977   Bioanalyzer electrophoresis system to validate the efficiency of rRNA removal using oligo-

978   dT. (A) Percent rRNA content in each RNA samples from 5 independently collected sets

979   of RNA. (B-E) Representative quantification curves of a sample set used to graph panel A.

980   Peaks corresponding to the expected sizes of 18S and 28S rRNA as labeled.

981

982
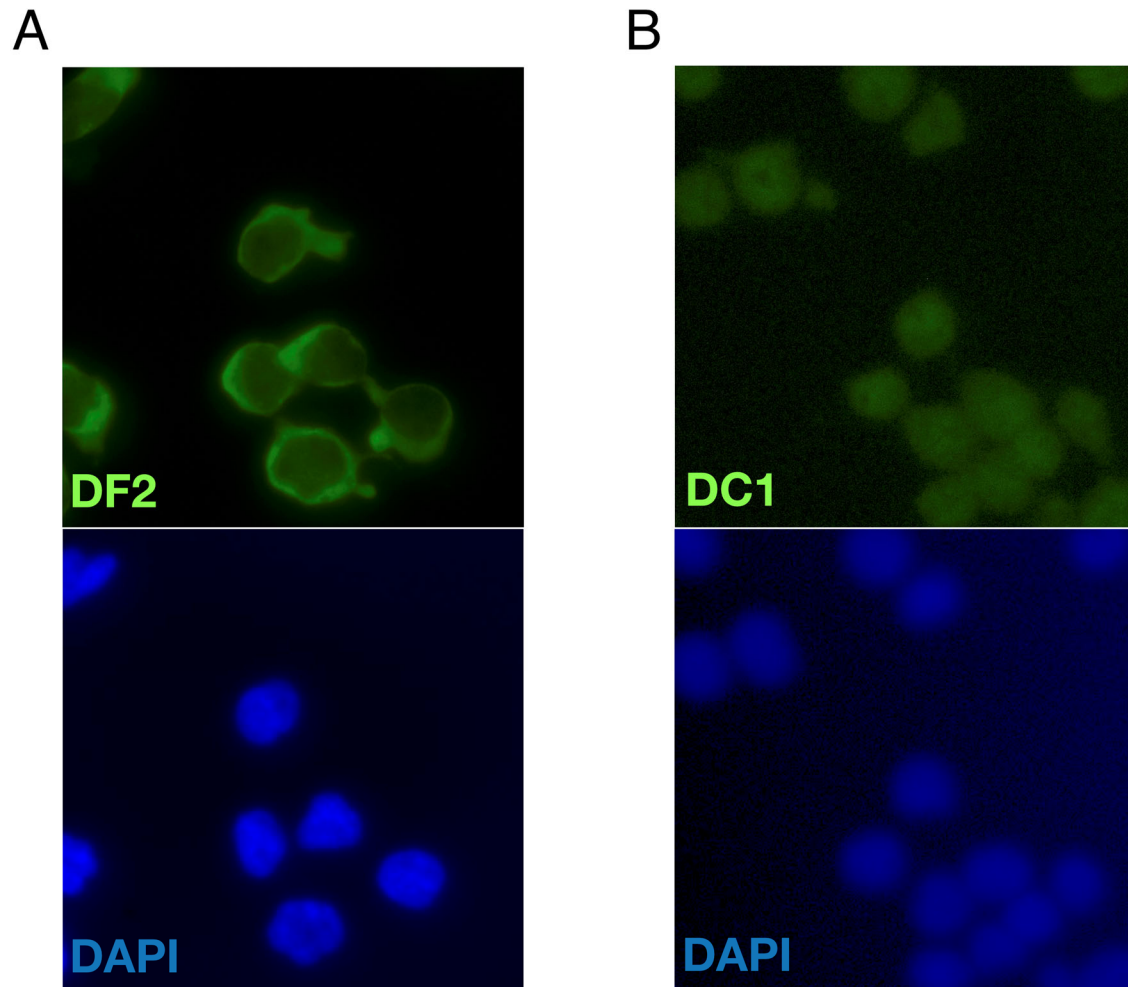
Fig. S2. Intracellular localization of m6A readers YTHDF2 and YTHDC1 in CD4+ T cell lines.

CEM-SS T cells were stained with antibodies targeting endogenous YTHDF2 (A) or YTHDC1 (B), co-stained with the nuclear stain DAPI, then visualized by fluorescence microscopy.